UDC 638.12+519.24 *https://doi.org/10.31861/biosystems2026.01.114*

CLASSIFICATION OF WING VENATION DEFORMITIES IN *APIS MELLIFERA* L. DRONES IN UKRAINE

O.V. CHEREVATOV[1], V.V. BABENKO[2], V.I. YAROVETS[2]

[1]*Yuriy Fedkovych Chernivtsi National University*
2 Kotsyubynskoho St., Chernivtsi, Ukraine, 58012
E-mail: o.cherevatov@chnu.edu.ua
[2]*Ivan Franko Lviv National University*
1 Universytetska St., Lviv, Ukraine, 79000
E-mail: bww04@ukr.net, 1951nadija@gmail.com

The aim of this study was to evaluate the potential of using information on wing venation distortions in drone Apis mellifera L. to infer properties of haploid genomes in the honey bee.

A total of 260 colonies and 30,821 drones were examined. Wing venation distortions and their localization were identified. Eleven distinct defect types were classified and denoted as <X>, where X ∈{A, B, …, K}. For a subset of 40 colonies, discriminant analysis and analysis of variance (ANOVA) were applied to cluster wings within colonies into two groups and to compare defect-free and defective wings belonging to the same cluster.

The proportions of defect types <F>, <C>, and <D> were 14.74%, 5.55%, and 2.68% of the total number of analyzed wings, respectively. In 78 (30%) colonies, the proportion of type <F> defects exceeded 20%. The frequencies of other defect types were substantially lower, ranging from 0.43% to 1.39%. However, individual colonies exhibiting high frequencies of defects <A> (up to 42%) and <B> (up to 34%) were identified. In addition to clearly expressed defects, the constant presence of weakly expressed anomalies (<<A>> and <<B>>) was detected, with a total frequency exceeding 40%.

When the proportion of clearly expressed deformities reaches or exceeds 23%, drone wing morphology can be employed to evaluate variation in genotype–phenotype correspondence between normal wings and wings exhibiting deformities.

Keywords: Honey bee, drones, wing venation defects, genome, haplodiploidy, plasticity, canalization, pleiotropy, analysis of variance, discriminant analysis

Introduction. Studies of phenotypic variability in insects aimed at elucidating mechanisms of adaptability and genetic robustness have a long history (Dobzhansky, 1951; Wagner et al., 1997; Rutherford et al., 1998) and continue to develop in contemporary research (Cabon et al., 2025). Various morphological structures of insect bodies can be used as objects of analysis (Zhang et al., 2025; Kim, 2021). Among these, wings are considered one of the most informative sources of phenotypic data (Mauser et al., 2025; Henriques et al., 2020). Due to its biological characteristics (high reproductive rate and relative ease of genetic manipulation), the fruit fly (*Drosophila melanogaster*) is most commonly used as a model organism (Chari et al., 2013).

The study of crossvein deformities in *Drosophila* wings formed the basis of classical experiments on heat shock-induced mutagenesis, which led to the establishment of "upward" and "downward" lines differing in the frequency of venation defects (Waddington, 1953). Subsequent crosses with wild-type individuals confirmed the heritable nature of this trait, which persisted even in the absence of the stressor. In contemporary studies, differences in the frequency of wing defects among *Drosophila* populations are used as indicators of developmental decanalization under environmental influences. For example, comparisons between Ethiopian and Zambian populations revealed significant phenotypic differences, including larger wing size in the former and a substantially higher frequency of abnormalities following induced mutagenesis (Lack et al., 2016). These data indicate a relationship between wing size and the frequency of venation defects, likely due to the action of multiple mutant alleles, and can be interpreted as evidence for genetic decanalization, with venation defects manifesting as pleiotropic effects.

Wing venation in the honey bee (*Apis mellifera*) is characterized by a high degree of stability and a species-specific structural pattern (Fig. 1).

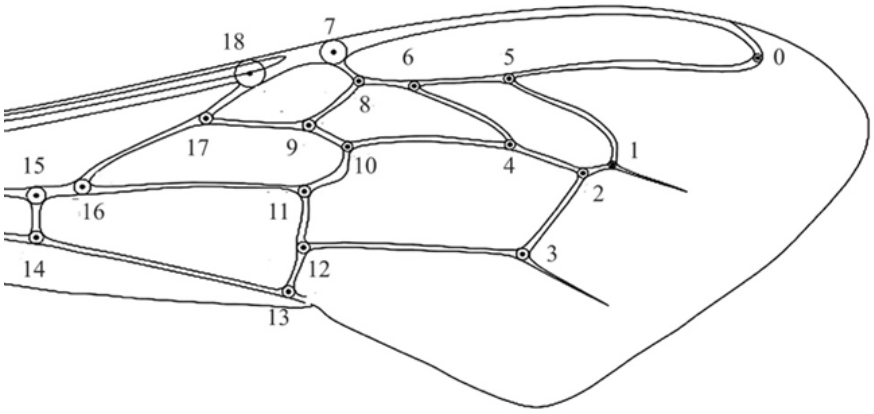

Fig.1. Typical wing venation pattern of Apis mellifera L. Dots and circles show the intersections of the veins, the so-called landmarks

Distortions in wing venation patterns of worker honey bees do occur; however, they are rare and do not exhibit a systematic character. In contrast, drones in *Apis mellifera* are haploid, and their wing venation displays a substantially higher level of defectiveness, both in the nature of distortions and in their frequency. This may indicate increased developmental instability. The authors are aware of only one work that examined anomalies of the venation of the forewings of worker bees and drones without attempting to classify them (Łopuch, et al., 2016). Unlike the studies discussed above, the present work examines phenotypic variability-primarily in natural ("wild") populations-without the use of induced mutagenesis. To this end, empirical data on drone wings of *Apis mellifera* exhibiting venation defects were systematized, and an attempt was made to relate venation defectiveness to phenotypic plasticity, canalization, and developmental stability. The interpretation of the results is based on analytical frameworks and conclusions derived from studies of *Drosophila melanogaster* wing morphology (Waddington, 1953; Pelletier et al., 2024). The authors consider the results obtained in this study to be preliminary and primarily exploratory. At the same time, the observed relationships between primary and pleiotropic morphological traits of the wing indicate their potential utility for investigating the properties of haploid genomes.

Materials and methods. To assess distortions in wing venation, a total of 30,821 drone wings from *Apis mellifera* L. populations distributed across the Lviv, Khmelnytskyi, Zhytomyr, Kyiv, Poltava, Kharkiv, and Sumy regions of Ukraine were examined. Right forewings were mounted on microscope slides using glycerol. High-resolution images were acquired using a ROSO M5 digital camera (50 MP) mounted on a stereomicroscope (MST 131, PZO Warszawa) at ×25 magnification. The images were stored in a digital database. Landmark placement and coordinate acquisition were performed according to the scheme shown in Fig. 1 using tpsDig2 software.

Drone wing morphology was analyzed within the framework of classical morphometrics using nine indices: Cubital index (Ci), Dumb-bell index (Dbi), Discoidal shift (Disc. sh.), Precubital index (Pci), and Radial index (Ri), following standard definitions (Bouga et al., 2011), as well as four indices proposed by the authors: Ci.1.1, Ci.2.1, Ci.2.2, and Ci.3. The latter were calculated as ratios of distances between landmarks: Ci.1.1=d(6,1)/d(5,4), Ci.2.1=d(10,4)/d(5,6), Ci.2.2=d(10,4)/d(8,6), Ci.3=d(9,17)/d(9,8), where $d(m,n)$ denotes the Euclidean distance between landmarks m and n (Fig. 1).

Statistical analyses were performed using the STATISTICA software package. Relationships between wing clusters and intra-cluster groups were evaluated using Mahalanobis distances (MD). An empirical similarity scale was applied as follows: MD = 0–2 indicates high similarity, 2.0–2.6 moderate similarity, 2.6–3.5 low similarity, and >3.5 indicates no similarity (Galatiuk et al., 2024). The robustness of the results was assessed using discriminant analysis and analysis of variance (ANOVA), based on Fisher's F-statistic and corresponding significance levels (p-values).

Results. A preliminary analysis of data collected between 2020 and 2025 revealed venation distortions in a substantial proportion of drone wings. The most characteristic and recurrent deviations from the normal pattern, including structural alterations and deformations, are presented in Figs. 2. The terminology used to describe venation distortions is consistent with that previously proposed for classifying wing defects in *Drosophila melanogaster*.

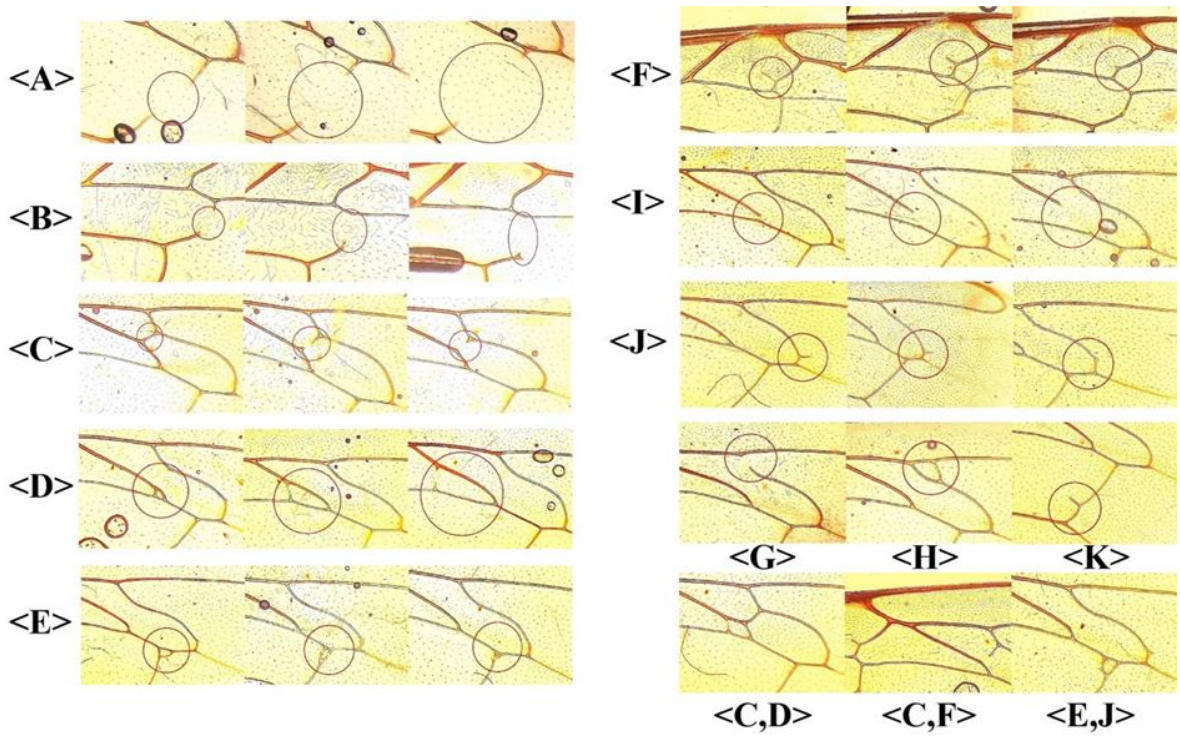

Fig. 2. Representative types of wing venation defects: – partial absence of cross-veins (cross-veins missing or incomplete), denoted as <A>, <B>; – absence of vein segments, potentially accompanied by the loss of vein intersection points (landmarks), denoted as <B>, <I>, <G>; – presence of additional veins not characteristic of the normal Apis mellifera wing pattern (ectopic cross-vein or extraneous vein material), denoted as <C>, <F>, <J>, <K>; – vein bifurcation leading to the formation of additional, atypical venation elements (extraneous vein material), denoted as <E>, <H>; – combined defects (co-occurrence of two or more defect types), denoted as <C,D>, <C,F>, <E,J>.

The original English terms are presented in italics following Lack et al. (2016): «*ectopic cross-vein*», «*cross-veins missing or incomplete*», and «*extraneous vein material*». Additional types of venation distortions were also observed; however, these occurred only sporadically and, with few exceptions, did not exceed 3% in frequency. Therefore, they were grouped under a single category (<Other>) and are not illustrated separately. To investigate potential relationships between primary morphological traits and defect types, representative colonies were selected with defect frequencies ranging from 22.8% to 66.67% (mean = 45.25%), and sample sizes ranging from 118 to 342 wings (mean = 212). Statistical analysis was performed using analysis of variance (ANOVA). The results are presented in Tables 4–5 and Figures 3–4. Colony identifiers correspond to queen identifiers.

Data on defects classified as <Other> (Table 4), with frequencies below 3%, were excluded from the analysis, as their low representation does not allow for statistically reliable inference.

Table 1.

General information on the number of honey bee colonies analyzed during 2020–2025. Data on the number, proportions, and types of venation defects are presented; proportions are expressed as percentages (%)

Number of colonies examined, N_{coloni}	Number of colonies where the proportion of defective wings $\omega>5\%$, N_{def}	Proportion of colonies where the proportion of defective wings $\omega>5\%$, N_{def}/N_{coloni}, %
260	256	98.46

Table 2.

Statistical summary of defect types and levels (<20% and >20%) at both colony and overall levels. Defect frequencies below 3% within colonies were excluded. The total number of colonies analyzed was N=260, with N = 30,821 wings examined, of which N=8,781 were classified as defective

Defect type and prevalence within colonies *	N**	N_{def}***	N_{def}/N_{sum}**** (%)	N_{def}/N_{sumdef}***** (%)
<A>, (<20%)	11	33	0.11	0.38
<A>, (>20%)	2	101	0.33	1.15
<B>, (<20%)	66	309	1.01	3.52
<B>, (>20%)	4	117	0.38	1.33
<C>, (<20%)	174	1158	3.77	13.19
<C>, (>20%)	15	548	1.78	6.24
<D>, (<20%)	166	809	2.63	9.21
<D>, (>20%)	1	15	0.05	0.17
<E>, (<20%)	41	98	0.32	1.12
<E>, (>20%)	0	0	0	0
<F>, (<20%)	141	1607	5.23	18.30
<F>, (>20%)	78	2923	9.51	33.29
<Other>, (<20%)	176	944	3.08	10.75
<Other>, (>20%)	3	119	0.39	1.36
Разом	-	8781	28.59	100

*Note: * – Labels <A>, <B>, <C>, <D>, <E>, <F> correspond to defect types illustrated in Fig. 2. The category <20% indicates low defect levels (5–20% defective wings per colony), whereas >20% indicates high defect levels (>20%); ** - number of colonies with defective wings; *** - number of wings by defect types in individual colonies; **** - wing lobes with defects, N_{sum}=30821; ***** - proportions of defective wings among all defective ones, N_{sumdef}=8781.*

Table 3.

General characteristics of the distribution of wings from 19 colonies into two clusters, taking into account distortions in wing venation. N(%) – number and proportion of wings

Colony, number *	Defect type**, N(%)	Defect type**, N(%)	Defect type**, N(%)	Defect type**, N(%)	Total wings with defects***, N(%)	Total wings, N(%)
2.1	no	<F>	<C>	–	(F,C)	
–	49(61.25)	21(26.25)	10(12.50)	–	31(38.75)	80(45.20)
2.2	no	<F>	<C>	–	(F,C)	
–	43(44.33)	28(28.87)	26(26.80)	–	54(55.67)	97(54.80)
5.1	no	<F>	<D>	<J>	(F,D,J)	
–	49(41.53)	35(29.66)	24(20.34)	10(8.47)	69(58.47)	118(55.14)
5.2	no	<F>	<D>	<J>	(F,D,J)	
–	34(35.42)	39(40.63)	10(10.42)	13(13.54)	62(64.58)	96(44.86)
6.1	no	<F>	–	–	–	
–	40(56.34)	31(43.66)	–	–	–	71(49.31)
6.2	no	<F>	–	–	–	
–	31(21.53)	42(29.17)	–	–	–	73(50.69)
10.1	no	<F>	<C>	<F,C>	(F,C)	
–	39(52.70)	10(13.51)	12(16.22)	13(17.57)	35(47.30)	74(42.77)
10.2	no	<F>	<C>	<F,C>	(F,C)	
–	53(53.54)	12(12.12)	19(19.19)	15(15.15)	46(46.46)	99(57.23)
14.1	no	<F>	–	–	–	
–	28(47.68)	31(52.54)	–	–	–	59(40.97)
14.2	no	<F>	–	–	–	
–	47(55.29)	38(44.71)	–	–	–	85(59.03)
17.1	no	<F>	<C>	<F,J>	<F,C>	
–	70(57.85)	7(5.79)	32(26.45)	6(4.96)	6(4.96)	121(43.21)
17.2	no	<F>	<C>	<F,J>	<F,C>	159(56.79)

–	119(74.84)	9(5.66)	24(15.09)	4(2.52)	3(1.89)	
18.1	no	<F>	<C>	<F,C>	(F,C)	
–	44(55.70)	11(13.92)	17(21.52)	7(8.86)	35(44.30)	79(50.97)
18.2	no	<F>	<C>	<F,C>	(F,C)	
–	56(73.68)	5(6.58)	13(17.11)	2(2.63)	20(26.32)	76(49.03)
20.1	no	<F,C,D,J>	–	–	–	
–	44(62.86)	26(37.14)	–	–	–	70(53.44)
20.2	no	<F,C,D,J>	–	–	–	
–	31(50.82)	30(49.18)	–	–	–	155(47.69)
22.1	no	<F>	–	–	–	
–	46(52.27)	42(47.73)	–	–	–	88(51.76)
22.2	no	<F>	–	–	–	
–	37(45.12)	45(54.88)	–	–	–	82(48.24)
26.1	no	<F>	<C>	<J>	(F,C,J,D)	
–	55(61.80)	12(13.48)	14(15.73)	6(6.38)	34(38.20)	89(48.63)
26.2	no	<F>	<C>	<J>	(F,C,J,D)	
–	72(76.60)	10(10.64)	1(1.06)	5(5.32)	22(23.40)	94(51.37)
31.1	no	<J>	<F>	<C>	<D>	
–	149(73.76)	29(14.36)	14(6.39)	6(2.97)	4(1.98)	202(59.06)
31.2	no	<J>	<F>	<C>	<D>	
–	115(82.14)	13(9.29)	6(4.29)	3(2.14)	3(2.14)	140(40.94)
32.1	no	<J>	–	–	–	
–	64(81.01)	15(18.99)	–	–	–	79(54.86)
32.2	no	<J>	–	–	–	
–	53(81.54)	12(18.46)	–	–	–	65(45.14)
87.1	no	<C>	<C,F>	<C,J>	(C,F,J)	
–	40(37.04)	19(17.59)	27(25.00)	22(20.37)	68(62.96)	108(64.29)
87.2	no	<C>	<C,F>	<C,J>	(C,F,J)	
–	17(28.33)	15(25.00)	13(21.67)	15(25.00)	43(71.67)	60(35.71)
D1.1	no	<B>	<C>	<J>	(B,C,J)	
–	81(54.73)	40(27.03)	11(7.43)	16(10.81)	67(45.27)	148(59.92)
D1.2	no	<B>	<C>	<J>	(B,C,J)	
–	41(41.41)	34(34.34)	19(19.19)	5(5.05)	58(58.58)	99(40.08)
D2.1	no	<C>	<F>	–	(F,C)	
–	97(57.06)	38(22.35)	35(20.59)	–	73(42.94)	170(52.31)
D2.2	no	<C>	<F>	–	(F,C)	
–	94(60.65)	31(20.00)	30(19.35)	–	61(39.35)	155(47.69)
S.1	no	<F>	–	–	–	
–	52(77.61)	15(22.39)	–	–	–	67(44.08)
S.2	no	<F>	–	–	–	
–	58(68.24)	27(31.76)	–	–	–	85(55.92)
P.1	no	<A>	–	–	–	
–	36(58.06)	26(41.94)	–	–	–	62(52.54)
P.2	no	<A>	–	–	–	
–	23(19.49)	33(27.94)	–	–	–	56(47.46)
K14.1	no	<F>	–	–	–	
–	95(66.90)	47(33.10)	–	–	–	142(41.64)
K14.2	no	<F>	–	–	–	
–	98(49.25)	101(50.75)	–	–	–	199(58.36)
X.1	no	<F>	<C>	–	(F,C)	
–	65(68.42)	22(23.16)	8(8.42)	–	30(31.58)	95(46.57)
X.2	no	<F>	<C>	–	(F,C)	
–	74(67.89)	26(23.85)	9(8.26)	–	35(32.11)	109(53.43)

*Note: * – the numbers 1 and 2 appearing after the dot in colony labels indicate cluster identifiers; ** – notation: <-> denotes wings without defects; <A>, <B>, <C>, <D>, <F>, <J> denote wings with specific defect types; combinations such as <F,C> or <F,C,D,J> indicate the simultaneous presence of multiple venation defects; *** – the sums of the wings of the wings with the corresponding combinations of types are taken into account: (F,C), (F,D,J), (C,F,J), (B,C,J), (F,C,J,D).*

Table 4.

Assessment of similarity between groups of drone wings with and without defects based on Mahalanobis distances and ANOVA

Clusters being compared*	MD	Fisher's criterion, *F*	*p*–level	Clusters being compared*	MD	Fisher's criterion, *F*	*p*–level
2.1no–2.1(F,C)	0.98	2.22**	0.0306**	2.2no–2.2(F,C)	1.12	3.39**	0.0013**
5.1no–5.1(F,D,J)	0.51	0.98	0.4604	5.2no–5.2(F,D,J)	1.17	3.17**	0.0024**
6.1no–6.1<F>	0.78	1.14	0.351	6.2no–6.2<F>	1.05	2.13**	0.039**
10.1no–10.1(F,C)	0.86	1.655	0.131	10.2no–10.2(F,C)	1.29	1.756**	0.097**
14.1no–14.1<F>	1.47	3.585**	0.0017**	14.2no–14.2<F>	0.90	1.419	0.195
17.1no–17.1(F,C)	0.89	2.87**	0.0045**	17.2no–17.2(F,C)	0.63	1.128	0.3464
18.1no–18.1(F,C)	0.87	1.40	0.2057	18.2no–18.2(F,C)	0.77	1.51	0.1632
20.1no–20.1<F,C,D,J>	0.78	0.95	0.486	20.2no–20.2<F,C,D,J>	0.93	1.59	0.22
22.1no–22.1<F>	1.22	3.94**	0.0004**	22.2no–22.2<F>	0.50	0.57	0.816
26.1no–26.1(F,C,D,J)	1.13	2.57**	0.0119**	26.2no–26.2(F,C,D,J)	1.04	2.32**	0.0217**
31.1no–31.1<J>	0.48	1.14	0.3381	31.2no–31.2<J>	0.77	1.24	0.2784
32.1no–32.1<J>	0.76	0.76	0.65	32.2no–32.2<J>	0.85	0.74	0.674
87.1no–87.1(C,F,J)	1.09	4.18**	0.0001**	87.2no–87.2(C,F,J)	1.31	2.63**	0.014**
D1.1no–D1.1(B,C,J)	0.60	1.56	0.1325	D1.2no–D1.2(B,C,J)	0.72	1.64	0.1164
D1.1no–D1.1<B>	0.69	1,53	0,1468	D1.2no–D1.2<B>	0.83	1.95	0,0606
D1.1no–D1.1<C>	1.22	2.25**	0.0265**	D1.2no–D1.2<C>	0.95	1.82	0,0870
D1.1no–D1.1<J>	0.99	1.69	0.1047	D1.2no–D1.2<J>	1.27	0.744	0,6668
D2.1no–D2.1(F,C)	0.98	2.22**	0.0306**	D2.2no–D2.2(F,C)	1.12	3.39**	0.0013**
S.1no–S.1<F>	1.11	1.691	0.119	S.2no–S.2<F>	0.87	1.290	0.254
P.1no–P.1<A>	1.65	3.78**	0.001**	P.2no–P.2<A>	1.72	4.01**	0.0008**
Kr14.1no–Kr14.1<F>	0.51	1.01	0.4354	Kr14.2no–Kr14.2<F>	0.61	1.62	0.1124
X.1no–X.1(F,C)	1.19	2.83**	0.0059**	X.2no–X.2(F,C)	0.62	0.95	0.4852

*Note: * – the notation <-> denotes wings without defects; <A>, <B>, <C>, <D>, <F>, <J> — denote specific defect types; <F,C,D,J> — corresponds to wings with a combination of corresponding defects; (F,C), (F,D,J), (B,C,J), (C,F,J), (F,C,D,J) — the sum of wings with all defects of the specified types is taken into account; numbers 1 and 2 following the dot in colony labels indicate cluster numbers; ** – Fisher's criterion values indicate statistically significant differences between variances: $F>F_{critical}$, $p<0.05$.*

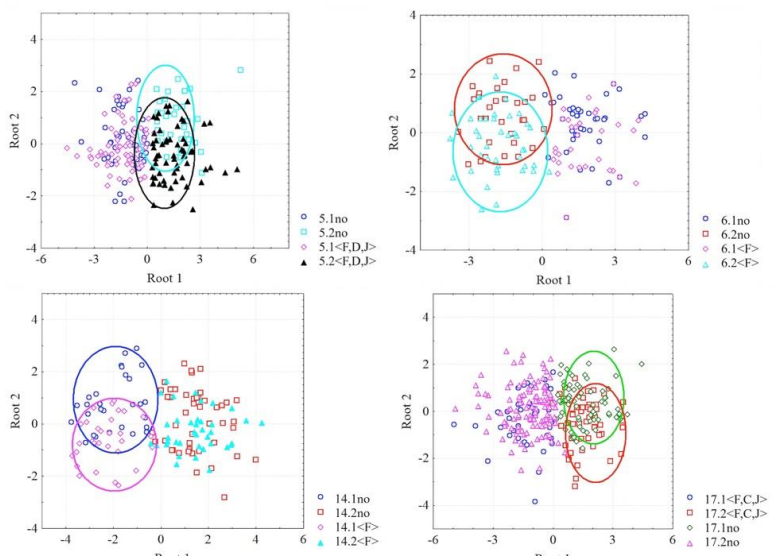

Fig. 3. Distribution of centroids of drone wing clusters for colonies No. 5, 6, 14, and 17 in the canonical variable space. Numbers 1 and 2 following the dot in colony labels indicate cluster identifiers. The notation "no" denotes wings without defects; <F> denotes wings with the corresponding defect type; (F,D,J) and (F,C,J) represent aggregated groups of wings with combinations of the specified defects.

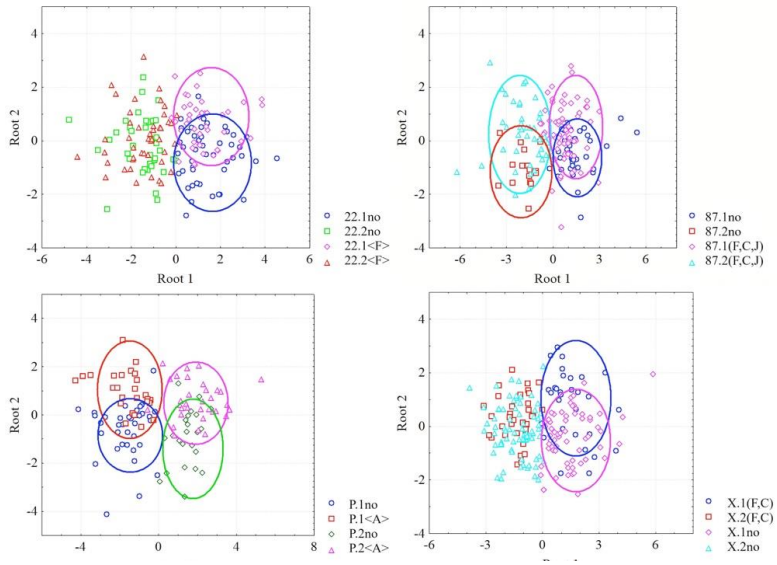

Fig. 4. Distribution of centroids of drone wing groups for colonies No. 22, 87, P, and X in the canonical variable space. Numbers 1 and 2 following the dot in colony labels indicate cluster identifiers. The notation: "no" denotes wings without defects; <A>, <F> denote wings with corresponding defect types; (C,F), (F,C,J) represent aggregated groups of wings with combinations of the specified defects

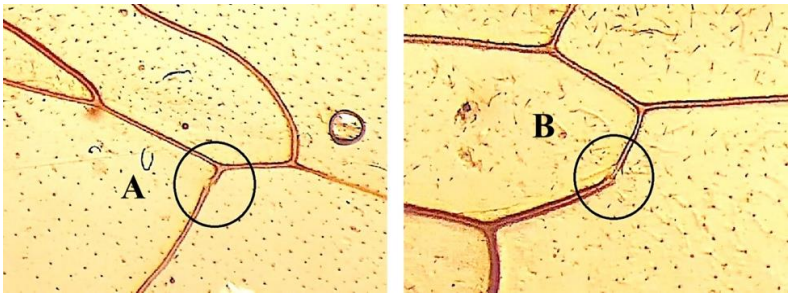

Fig. 5. Manifestation patterns of weakly expressed venation defects of types <A> and <B> in drone wings. These defects are classified as subtle and are denoted by refined symbols <<A>> and <<B>>.

Discussion. Although the venation pattern of drone wings is considerably more complex than that of *Drosophila*, most types of venation distortions are similar in nature, and their occurrence is spatially localized. This made it possible to classify the most frequently observed and clearly expressed defects into distinct types (Figs. 2).

Of the 260 colonies examined in the present study, only four showed no defects in drone wing venation patterns. In 256 colonies (98.46%), the overall proportion of defective wings exceeded 5%. This proportion may be considered an indicator that the factors underlying alterations in wing venation patterns are of substantial significance. The division of colonies into two groups—those with more than 20% and less than 20% defective wings—is conditional and was introduced to ensure a sufficient sample size of defective wings for statistically robust analysis (Table 3).

It was established that the proportions of defects of types <F>, <C>, and <D> accounted for 14.7%, 5.54%, and 2.67%, respectively, of the total number of analyzed wings. In 78, 15, and 1 colonies, respectively, the proportion of defective wings exceeded 20%. The frequencies of other defect types (<A>, <B>, <E>, <G>, <H>, <I>, <J>) were substantially lower, ranging from 0.43% to 1.39% of the total number of wings. However, isolated cases of high defect prevalence were observed, for example, for type <A>, where the proportion exceeded 42%.

To investigate relationships between groups of normal and defective wings in greater detail, 40 colonies (80 wing clusters) were analyzed. The most representative results are presented for 19 colonies (Tables 3, 4; Figs. 3, 4). For the remaining 21 colonies, no differences between normal and defective wing groups were detected; therefore, these results are not shown.

For the majority of analyzed clusters (63; 78.75%), no differences were found between groups of defective and non-defective wings. In colonies where such differences were observed, the proportion of defective wings ranged from 23% to 67% (mean: 45%). Colonies with a high proportion of defective wings typically exhibited multiple defect types, most of which were represented at low frequencies. However, one, and less frequently two, defect types tended to predominate. This pattern was observed for queens Nos. 5, 6, 14, 22, 32, S, K14, and X, where defects of type <F> were dominant; for no. 17 — type <C>; no. 32 — type <J>; and no. P — type <A>. In queens nos. 2, 10, 26, and 87, different defect types were present in approximately equal proportions.

In cases where the total proportion of defects classified as <Other> did not exceed 3%, the corresponding wing images were excluded from analysis. When assessing relationships between normal and defective wing groups, all clearly expressed defect types were analyzed jointly, which allowed statistically robust results to be obtained.

For queens nos. 18, 20, 31, 32, D1, S, and K14, the phenotypes of wing groups with and without defects within both clusters do not exhibit statistically significant differences: Mahalanobis distances (MD) between centroids range from 0.48 to 1.11, indicating a high degree of morphological similarity. In combination with ANOVA results (no significant differences: $F \leq F_{critical}$, $p \geq 0.05$), these cases should be interpreted as manifestations of effective developmental canalization, in which variation associated with venation defects does not result in systematic shifts within the multivariate morphospace. In contrast, for queens nos. 2, 26, 87, D2, and P, statistically significant differences between defective and non-defective wing groups are observed within clusters: MD values range from 0.98 to 1.72, and ANOVA results confirm rejection of the null hypothesis ($F > F_{critical}$, $p < 0.05$). It is critical to emphasize that MD values alone are insufficient for inference; however, when combined with the results of the analysis of variance, they indicate coordinated morphological shifts. These cases can be interpreted as instances of decanalization, in which developmental perturbations are associated with directional changes in phenotype rather than merely increased stochastic variance. For queens nos. 5, 6, 10, 14, 17, 22, and X, a heterogeneous pattern is observed: within a given colony, one cluster may show similarity between defective and non-defective wings, while the other exhibits significant differences. The spatial arrangement of centroids in canonical space (Figs. 3, 4) supports this asymmetry: centroid shifts are evident in some pairs (e.g., 5.2↔5.2(F,D,J), 6.2↔6.2<F>, 14.1↔14.1<F>, 17.1↔17.1(F,C,J), 22.1↔22.1<F>, 87.1↔87.1(F,C,J), 87.2↔.2(F,C,J), P.1↔P.1<A>, P.2↔P.2<A>, X.1↔X.1(F,C)), whereas no shift is observed in others (5.1↔5.1(F,D,J), 6.1↔6.1<F>, 14.2↔14.2<F>, 17.2↔17.2(F,C,J) (Fig.3), 22.2↔22.2<F>, X.2↔X.2(F,C) (Fig.4)). This pattern is consistent with the notion that different haploid genomes expressed within a single colony may differ in their degree of canalization. The displacement of centroids for defective wings relative to non-defective ones should be interpreted as a directional shift in multivariate trait space rather than random variation. This suggests that venation defects are associated with coordinated morphological changes,

rather than representing purely local developmental anomalies. Within the framework of canalization theory, such patterns are indicative of decanalization, reflecting reduced phenotypic robustness and increased sensitivity to genetic or environmental perturbations. However, interpreting these shifts as evidence of "genomic plasticity" requires caution. Plasticity implies adaptive phenotypic responsiveness to environmental variation, whereas the observed effects may also reflect developmental instability or cumulative mutational load. As emphasized by Pesevski et al. (2020), the relationship between trait means, variances, and frequency of abnormal phenotypes is complex and governed by polygenic architectures.

An important factor determining both the frequency and the spectrum of wing venation defects is the action of stress factors (Gillis et al., 2019; Sagastume et al., 2025). Reaching critical levels of such factors is associated with increased phenotypic variability and can be interpreted as developmental decanalization in the sense of Waddington's concept. For colonies with a long history of selection, one potential source of this effect may be inbreeding (Kim, 2021); however, the present study demonstrates a statistically detected association rather than a proven causal relationship. In the overall dataset, type <A> defects occur at a low frequency (<0.33% of all wings and <2.64% of defective wings; Table 3). At the same time, for the colony headed by queen No. P [DE-6-115-19-2019 (17-2-112/17 × 11-208-79/2015K), breeder: S. Rausch], a consistently high prevalence of this defect is observed (63% without defects / 37% with defect <A>), which remains stable across subsequent generations. Such stability is unlikely to result from random variation and instead suggests reduced canalization buffering and increased penetrance of genetic factors affecting wing development. In this context, wing defects should be interpreted as pleiotropic manifestations of underlying genetic variation influencing developmental pathways. Similarly, in specific colonies (Table 5), shifts toward rare defect types (<B>, <J>) were observed, indicating possible local decanalization driven by particular combinations of genomic background and environmental conditions. In open populations, where directional selection pressure is reduced or absent, a different pattern emerges: the dominance of a single defect type (<F>) alongside relatively stable frequencies of other defects. This is consistent with partial canalization, in which developmental systems remain generally robust but retain specific "weak points" within the genomic architecture.

The attempt to relate defect frequency to a primary morphological trait follows the framework proposed by Waddington (1953). Within classical morphometrics, "cluster morphology" can be treated as an empirical representation of a phenotype associated with a haploid drone genome. The haploid nature of drones enhances the interpretability of genotype–phenotype relationships compared to diploid worker bees.

Mahalanobis distances between clusters (MD = 2.18–3.2) correspond to moderate or low similarity according to the adopted empirical scale. Although this does not constitute a criterion for statistical significance, it does indicate morphological differentiation between clusters. Under such conditions, differences in the frequency and types of defects between clusters might be expected. However, the results demonstrate that defective wings are distributed approximately evenly between clusters. This suggests that the mechanisms underlying defect formation are not phenotype-specific but instead reflect a complex interplay of polygenic architecture, pleiotropic effects, and genome–environment interactions.

Within the proposed interpretative framework, significant differences between normal and defective wings indicate decanalization and phenotypic plasticity, whereas the absence of such differences-even at high defect frequencies-indicates effective canalization accompanied by developmental stability. The estimate that approximately 21% of haploid genomes exhibit adaptive potential should be regarded as an operational result derived from the applied morphometric framework rather than a universal biological constant. Similarly, the 23–67% defect range should be interpreted as an empirical indicator of conditions under which genomic plasticity may be detectable, rather than as a strict biological threshold.

The distortions presented in Figs. 2 and Tables 2–3 are clearly expressed and represent substantial deviations from the normal venation pattern of drone wings. At the same time, subtle distortions were also observed, typically corresponding to early-stage manifestations of defects (Fig. 5) that did not reach full morphological expression. For this reason, they were excluded from the overall defect statistics. Across most studied apiaries, the proportion of wings exhibiting such subtle defects ranged from 40% to 50%, while in some cases it exceeded 80%. This allows these features to be interpreted as a stable "defect background" or low-intensity morphological noise. To distinguish these subtle forms from typical defects of types <A> and <B>, refined notations <<A>> and <<B>> were introduced. The high prevalence of these subtle

defect types across all studied colonies suggests that they represent a systematic component of phenotypic variability.

Conclusion. It has been demonstrated that wing venation defects, considered as manifestations of pleiotropic effects, enable the detection of differences between groups of wings within individual clusters, the morphology of which is determined by one of the two haploid genomes of the queen. It was established that the type of defect does not significantly influence the results of comparisons between groups of wings with and without defects.

The high frequency of defects of types <F>, <<A>>, and <<B>> indicates the presence of "vulnerable" regions within the genomic architecture that tend to manifest more frequently than other defect types under similar conditions.

The identification of individual colonies with a high proportion of defects of types <A> and <B>, which typically occur at frequencies below 5%, suggests the presence of stress factors that, under certain conditions, reach critical levels and significantly affect genome functioning.

Adherence to ethical principles. *The requirements of the recommendations of the EU Directive 2010/63/EU on the protection of animals used for scientific purposes have been met.*

Conflict of interest. *The authors declare no conflict of interest.*

Financing. *This study was not financed by any specific grant from financing institutions in the state, commer- cial, or non-commercial sectors.*

References:

1. Bouga, M., Alaux, C., Bienkowska, M., Büchler, R., Carreck, N.L., Cauia, E., Chlebo, R., Dahle, B., Dall'Olio, R., De la Rúa, P., Gregorc, A., Ivanova, E., Kence, A., Kence, M., Kezic, N., Kiprijanovska, H., Kozmus, P., Kryger, P., Le Conte, Y., Lodesani, M., Murilhas, A. M., Siceanu, A., Soland, G., Uzunov, G., Wilde, J. (2011). A review of methods for discrimination of honey bee populations as applied to European beekeeping. *J Apic Res*, 50(1), 51–84. https://doi.org/10.3896/IBRA.1.50.1.06
2. Cabon, L., Varma, M., Winter, G., Ebeling, A., & Schielzeth, H. (2025). Phenotypic plasticity, heritability, and genotype-by-environment interactions in an insect dispersal polymorphism. *BMC ecology and evolution*, *25*(1), 94. https://doi.org/10.5061/dryad.18931zd4t.
3. Chari, S., & Dworkin, I. (2013). The conditional nature of genetic interactions: the consequences of wild-type backgrounds on mutational interactions in a genome-wide modifier screen. *PLoS genetics*, 9(8), e1003661. https://doi.org/10.1371/journal.pgen.1003661
4. Dobzhansky, T. (1951). Race and humanity. *Science (New York, N.Y.)*, 113(2932), 264–266. https://doi.org/10.1126/science.113.2932.264
5. Gillis, M. K., & Walsh, M. R. (2019). Individual variation in plasticity dulls transgenerational responses to stress. *Funct Ecol*. 33, 1993–2002. https://doi.org/10.1111/1365-2435.13409
6. Henriques, D., Chavez-Galarza, J., Teixeira, J. S. G., Ferreira, H., Neves, C. J., Francoy, T., Pinto, M. A. (2020). Wing geometric morphometrics of workers and drones and single nucleotide polymorphisms provide similar genetic structure in the Iberian honey bee (Apis mellifera Iberiensis). *Insects*, 11(2), 89. http://dx.doi.org/10.3390/insects11020089
7. Kim, B.-J. (2021). Negative effects of inbreeding of artificially bottlenecked Drosophila melanogaster populations. *Proceedings of the national institute of ecology of the republic of korea*, *2*(2), 108–113. https://doi.org/10.22920/PNIE.2021.2.2.108
8. Lack, J. B., Monette, M. J., Johanning, E. J., Sprengelmeyer, Q. D., & Pool, J. E. (2016). Decanalization of wing development accompanied the evolution of large wings in high-altitude Drosophila. *Proceedings of the National Academy of Sciences*, 113, 1014–1019. https://doi.org/10.1073/pnas.1515964113
9. Łopuch, S., & Tofilski, A. (2016). The relationship between asymmetry, size and unusual venation in honey bees (Apis mellifera). *Bulletin of entomological research*, 106(3), 304–313. https://doi.org/10.1017/S0007485315000784
10. Mauser, K. M., Paudel, S., Sigmund, O., Entling, M. H., Ott, J., & Brühl, C. A. (2025). Effects of chemical and hydrological stress on the wing morphology of a damselfly, *Environmental Entomology*, nvaf112, https://doi.org/10.1093/ee/nvaf112
11. Pelletier, K., Bilodeau, M., Pellizzari-Delano, I., Siemon, M. D., Huang, Y., Pool, J. E. & Dworkin, I. (2024). Polygenic architecture of adaptation to a high-altitude environment for Drosophila melanogaster wing shape and size. *bioRxiv, preprint*. http://dx.doi.org/10.1101/2024.02.08.579525
12. Pesevski, M., & Dworkin, I. (2020). Genetic and environmental canalization are not associated among altitudinally varying populations of Drosophila melanogaster. *Evolution; international journal of organic evolution*, 74(8), 1755–1771. https://doi.org/10.1111/evo.14039
13. Sagastume, S., Cilia, G., Henriques, D., Yadró, C., Corona, M., Higes, M., Pinto, M. A., Nanetti, A., & Martín-Hernández, R. (2025). Climate change-induced stress in the honey bee *Apis mellifera* L.- a genetic review. *Frontiers in Physiology*, 16, 1623705. https://doi.org/10.3389/fphys.2025.1623705
14. Waddington, C. H. (1953), Genetic assimilation of an acquired character. *Evolution*, 7, 118-126. https://doi.org/10.1111/j.1558-5646.1953.tb00070.x
15. Wagner, G. P., Booth, G., & Bagheri-Chaichian, H. (1997). A population genetic theory of

canalization. *Evolution; international journal of organic evolution*, 51(2), 329–347. https://doi.org/10.1111/j.1558-5646.1997.tb02420.x
16. Zhang, X., Lu, J., Qu, X., & Chen, X. (2025). An Evaluation of Morphometric Characteristics of Honey Bee (Apis cerana) Populations in the Qinghai–Tibet Plateau in China. *Life*, 15(2), 255. https://doi.org/10.3390/life15020255

КЛАСИФІКАЦІЯ ДЕФОРМАЦІЙ У ЖИЛКУВАННІ КРИЛ ТРУТНІВ *APIS MELLIFERA* L. В УКРАЇНІ

О.В. ЧЕРЕВАТОВ[1], В.В. БАБЕНКО[2], В.І. ЯРОВЕЦЬ[2]

[1] *Чернівецький національний університет ім. Юрія Федьковича*
вул. Коцюбинського, 2, м.Чернівці, Україна, 58012
E-mail: o.cherevatov@chnu.edu.ua
[2] *Львівський національний університет ім. Ів.Франка*
вул. Університетська, 1, м. Львів, Україна, 79000
E-mail: bww04@ukr.net, 1951nadija@gmail.com

Метою роботи є оцінка можливості використання інформації про спотворення жилкування крил трутнів Apis mellifera L. для встановлення властивостей гаплоїдних геномів медоносної бджоли.

Досліджено 260 колоній і 30821 трутня. Виявлено спотворення жилкування крил та визначено їх локалізацію. Проведено типування 11 чітко виражених дефектів, які позначено у вигляді <X>, де X ∈ {A, B, …, K}. Для 40 колоній із використанням дискримінантного та дисперсійного аналізів виконано кластеризацію крил у межах колоній (на два кластери) та порівняння груп крил без дефектів і з дефектами, що належать до одного кластера.

Встановлено, що частки дефектів типів <F>, <C> та <D> становлять 14,74%, 5,55% і 2,68% відповідно від загальної кількості досліджених крил. У 78 (30%) колоніях частка дефектів типу <F> перевищує 20%. Частки інших типів дефектів є значно меншими і становлять 0,43–1,39%. Водночас виявлено окремі колонії з високою часткою дефектів типів <A> (до 42%) та <B> (до 34%). Окрім виражених дефектів, встановлено постійна наявність слабко виражених аномалій (<<A>> та <<B>>), сумарна частка яких перевищує 40%.

За умови, що частка чітко виражених дефектів становить ≥23%, морфологія крил трутнів може бути використана для оцінювання варіативності у відповідності генотипу та фенотипу між крилами без дефектів і з дефектами.

Ключові слова: Бджола медоносна, трутні, дефекти жилкування крил, геном, гаплодиплоїдність, пластичність, каналізація, плейотропія, дисперсійний аналіз, дискримінантний аналіз

Отримано редколегією 18.05.2026 р.
Підписано до друку 15.06.2026 р.
Дата публікації 30.06.2026 р.

ORCID ID
Олександр Череватов: https://orcid.org/0000-0003-0746-1208
Володимир Бабенко: https://orcid.org/0000-0002-4278-6473
Володимир Яровець: https://orcid.org/0000-0001-7083-8130